Transverse-size critical exponent of directed percolation from Yang-Lee zeros of survival probability

Milan Knežević [*]

Faculty of Physics, University of Belgrade, POB 368, 11001 Belgrade, Serbia

Miloš Knežević

Institut für Theoretische Physik, Technische Universität Berlin, Hardenbergstraße 36, D-10623 Berlin, Germany

By using transfer-matrix method we compute survival probabilities for the directed percolation problem on strips of a square lattice, and get very precise estimates of their Yang-Lee zeros lying closest to the real axis in the complex plane of occupation probability. This allows us to get accurate values for transverse-size critical exponent and percolation threshold.

I. INTRODUCTION

A close connection between the zeros of the partition function in the complex plane of an appropriate control parameter and the onset of phase transition was first pointed out by Yang and Lee [1,2]. It was shown that the loci of these zeros have a simple structure for many important models of equilibrium statistical mechanics. For a model with discrete energy levels, partition function can be expressed as a polynomial with positive coefficients, so that its zeros occur in complex-conjugate pairs or they lay on the negative real axis of pertinent complex plane, while the positive part of real axis is free of zeros for a finite system. For a large but finite system, the pairs of complex-conjugate zeros lying closest to the positive real axis (to be referred to as first zeros) are of special interest, since they exert direct influence on the onset of phase transition. According to this picture, singular behavior of the partition function and its derivatives can develop only in the thermodynamic limit, provided that some of its zeros in this limit tend towards the positive real axis, and the associated phase transition point emerges as an accumulation point of these zeros [1,2]. Soon after publication of their works, the Yang-Lee (Y-L) approach was adopted as a valuable tool in investigation of phase transitions, and it was used in many different studies, especially in the case of spin model systems (see, e.g., Refs. [3,4] for a review of early studies, and Ref. [5] for an account of more recent works). In addition, the Y-L approach has been successfully applied to some other models of equilibrium statistical physics, such as those relevant to polymer phase transitions [6–13], or simple models of biological interest [14,15].

To the best of our knowledge, there is no rigorous proof for the applicability of the Y-L approach to the case of statistical systems out of equilibrium. Nevertheless, the method has been successfully tested on certain examples of nonequilibrium steady-state phase transitions [5,16], first on simple models,

such as those describing driven diffusive [17–19], reaction-diffusion [20], and directed percolation processes [21,22]. Subsequently, the Y-L strategy has been extended and applied to a variety of more complex models, including quantum systems [23,24]. Recently, interest for this methodology has been further enhanced, due to the fact that Y-L zeros of some real physical systems can be accessed experimentally [25–30].

Directed percolation process has attracted a lot of attention over the past two decades, mainly due to the fact that a wide range of simple models of nonequilibrium processes having a transition into an absorbing state share the directed percolation universality class [31]. As we mentioned above, directed percolation problem was one of the first examples of a nonequilibrium system where the Y-L approach was proven to be successful [21,22]. These authors derived analytical expressions for a sequence of finite-time survival probabilities on a square lattice, and they provided clear numerical evidence that the first zeros of these functions, in the complex plane of associated occupation probabilities, indeed approach corresponding real axis as the system evolves in time. In this way, they were able to obtain rather good estimates not only for percolation thresholds, both for bond and site percolation problem, but also an estimate of universal longitudinal-size critical exponent; transverse-size critical exponent has not been examined in these works.

While the approach used in Refs. [21,22] is well suited for the calculation of longitudinal-size exponent in the framework of Y-L formalism, it is less convenient for studying percolation cluster sizes in the transverse direction. This motivated us to reconsider the problem of two-dimensional directed percolation by using a strip geometry, which allows us to control the perpendicular cluster size as well. Since the object of our main interest here is the transverse-size critical exponent, we focus our attention on the case of very long percolation clusters confined on strips of a fixed width n.

Using transfer-matrix approach we construct (numerically) exact expressions for the survival probabilities of the site-directed percolation on the strips of a fixed width and arbitrary length on the square lattice. Then a numerical analysis of the

_____
[*]knez@ff.bg.ac.rs
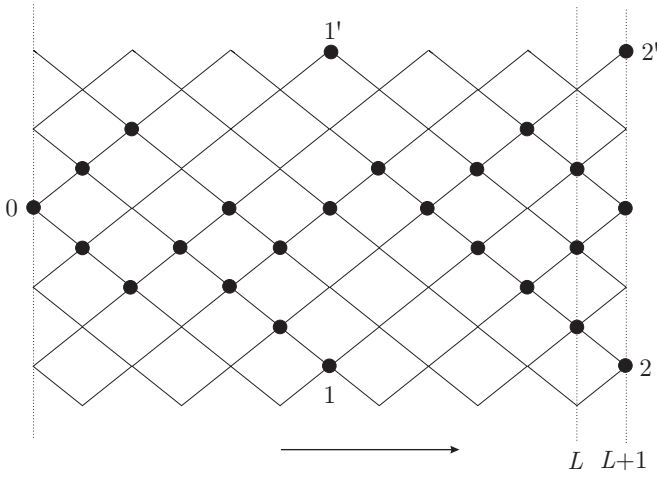
FIG. 1. Directed percolation cluster on the square lattice, made of 23 sites on a strip of width $n = 4$. Note that the sites denoted by 1 and 1′, as well as 2 and 2′, are, in fact, the same due to periodic boundary conditions applied along the vertical axis. The site at the root is denoted by 0 and the arrow indicates the preferred direction.

first zeros of these functions, combined with a simple scaling law, enables us to get estimates for the critical percolation probability and the transverse-size critical exponent. It is perhaps surprising that the precision of transverse-size critical exponent is comparable with precision of the best currently available estimates, although we worked on strips of reasonably small widths (for widths going up to $n = 19$). Extension of this work to larger strips is possible, but the calculation becomes a time-consuming process for larger values of n (to be discussed later). In any case, besides corroborating the general utility of the Y-L method for directed percolation revealed previously, our computation on strips shows that it can be quite competitive with other approaches aimed at getting accurate values of critical exponents.

The paper is organized as follows. In Sec. II we present our model, define some quantities of interest, and briefly describe the transfer-matrix approach on strips. In Sec. III we describe some details of our numerical approach and give the main results. In Sec. IV we give an outline of our approach, together with a summary of the obtained results.

II. MODEL

In this paper we consider statistical properties of directed percolation clusters on strips of the square lattice with periodic boundary conditions shown in Fig. 1. In a static interpretation that we use here, the preferred direction is a spatial direction (indicated by the arrow in Fig. 1) so that any site of the cluster can be reached from the site lying in the first column (root) by a path that never goes opposite to this direction. In the dynamical interpretation of directed percolation mentioned above, the preferred direction is time, so that to a cluster spanning the lattice of length L corresponds the evolution time equal to L.

We assume that each lattice site is present with occupation probability p and that it is absent with probability $q = 1 - p$. In contrast to the case of usual isotropic percolation, directed

percolation clusters display elongation along the preferred direction and shrinking in the transverse direction. As a consequence of this, metric properties of such clusters are best described in terms of two characteristic lengths $\xi^\parallel$ and $\xi^\perp$ for longitudinal and transverse directions, respectively. It is widely accepted that, near the critical occupation probability p_c (percolation threshold) of an infinite system, these lengths follow the power-law behavior: $\xi^\parallel \sim (p - p_c)^{-\nu^\parallel}, \xi^\perp \sim (p - p_c)^{-\nu^\perp}$, where $\nu^\parallel$ and $\nu^\perp$ are the universal longitudinal and transverse-size critical exponents, respectively.

Main quantity of interest in the percolation problem on strips is the survival probability $\mathcal{P}_{L,n}(p)$ that there is at least one spanning cluster going from the root to the Lth column for a given n. The probability $\mathcal{P}_{L,n}(p)$ can be expressed as a linear combination of a finite number of restricted probabilities $P_{L,n}(\mathcal{C}_i)$, where $P_{L,n}(\mathcal{C}_i)$ is the probability of the spanning cluster of length L ending with a given site configuration $\mathcal{C}_i$. Let us note that in our diagonal formulation of directed percolation problem these configurations refer to sites situated on a straight line passing through the vertical diagonals of lattice cells, as depicted in Fig. 1. The width n of the strip is equal to the number of vertices lying on this vertical line. The total number of site configurations for a strip of width n is obviously equal to $2^n - 1$ (if one omits the configuration with all empty sites). The transfer-matrix approach is based on the fact that one can express the probabilities $P_{L+1,n}(\mathcal{C}_k)$ in terms of $P_{L,n}(\mathcal{C}_i)$ via a set of $2^n - 1$ linear recursion relations.

The number of recursion relations can be significantly reduced by using symmetries of the system. Indeed, in addition to reflection symmetry with respect to a given point, in the case of periodic boundary conditions rotational symmetry is present as well. Owing to the presence of these symmetries one can classify configurations and make a partition of the whole set of possible configurations into $\mathcal{N} = \mathcal{N}(n)$ mutually disjunct subsets (classes), such that any configuration of a given subset can be related to any other configuration of the same subset by a combination of symmetry operations. Since all members of a given class of configurations are equivalent, one can take any of them to represent the whole class, which allows one to write a reduced system of linear recursion relation

$$P_{L+1,n}(\mathcal{C}_k) = \sum_{i=1}^{\mathcal{N}} \mathbf{M}_{ki}(p) P_{L,n}(\mathcal{C}_i), \tag{1}$$

where index i goes over different classes. To obtain the matrix element $\mathbf{M}_{ki}(p)$ of the transfer matrix $\mathbf{M}$, one considers a fixed configuration $\mathcal{C}_k$ at column $L + 1$ and selects all those configurations, lying at the Lth column, and belonging to the class of configuration $\mathcal{C}_i$ that ensure the connectivity of each occupied site lying at the right column (see Fig. 1). Then one associates the weight $p^s q^t$ to each allowed pair of configurations, where s is equal to the number of all occupied sites in the right column, and t is the number of those empty sites in the same column having at least one occupied predecessor (nearest-neighbor occupied vertex) at the left column. For small n all these matrix elements can be obtained by hand. For larger values of n one needs a computer code to construct $\mathbf{M}$, since its size $\mathcal{N} \times \mathcal{N}$ still grows exponentially but more slowly than $2^n \times 2^n$ (for example, we find $\mathcal{N}(20) = 27011 \ll 2^{20} \approx 10^6$).
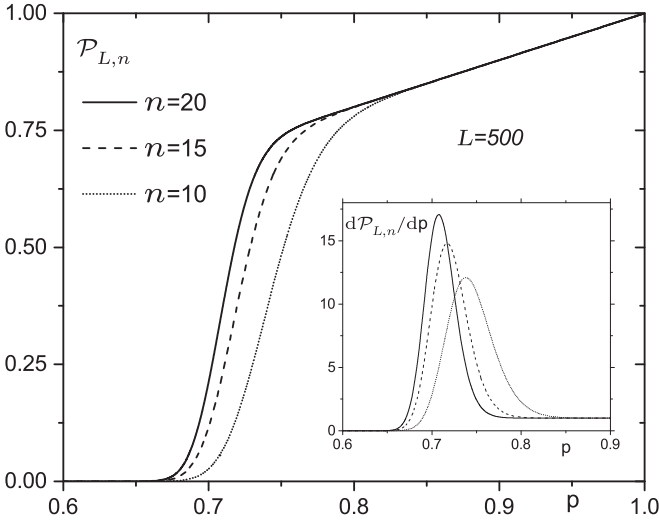
FIG. 2. Survival probabilities as function of the real occupation probability $0.6 \leqslant p \leqslant 1$ on strips of the square lattice of the length $L = 500$ and three different values of n. Derivatives of these functions with respect to p, for the same values of L and n, are presented in the inset.

For a fixed n, all column states, described through the set of restricted probabilities, are determined by the root state only,

$$\mathbf{P}_L = \mathbf{M}^L \mathbf{P}_0, \tag{2}$$

where $\mathbf{P}_L$ and $\mathbf{P}_0$ denote state vectors whose components are restricted probabilities corresponding to the Lth column and to the root, respectively. As a simple example, in Appendix we depicted the set of seven column states required for description of site-directed percolation on strips of width $n = 5$; corresponding transfer-matrix and state vectors are given in the same place. In our calculation we usually take that the root site is present with probability 1, but this choice is not essential since $\mathbf{P}_L$ is practically independent of initial conditions in the limit $L \gg 1$.

It is easy to see that the survival probability $\mathcal{P}_{L,n}(p)$ can be expressed as a linear combination of restricted probabilities

$$\mathcal{P}_{L,n}(p) = \sum_{i=1}^{\mathcal{N}} d(\mathcal{C}_i) P_{L,n}(\mathcal{C}_i), \tag{3}$$

where $d(\mathcal{C}_i)$ is the number of different configurations belonging to the class $\mathcal{C}_i$, or, to say it in simple terms, $d(\mathcal{C}_i)$ is the number of ways the configuration of type $\mathcal{C}_i$ can be embedded in a column of width n. It is also obvious that these numbers must satisfy the following sum rule $\sum_{i=1}^{\mathcal{N}} d(\mathcal{C}_i) = 2^n - 1$.

To get a feeling on the shape of percolation probability for clusters confined to strips (in fact, cylinders), we computed $\mathcal{P}_{L,n}(p)$ numerically for three representative values of n and a fixed value of L (see Fig. 2). Derivatives of these functions are presented in the inset of the same figure. Note that the height of the maxima of $d\mathcal{P}_{L,n}(p)/dp$ grows up, while their position moves slowly towards the smaller values of p, by
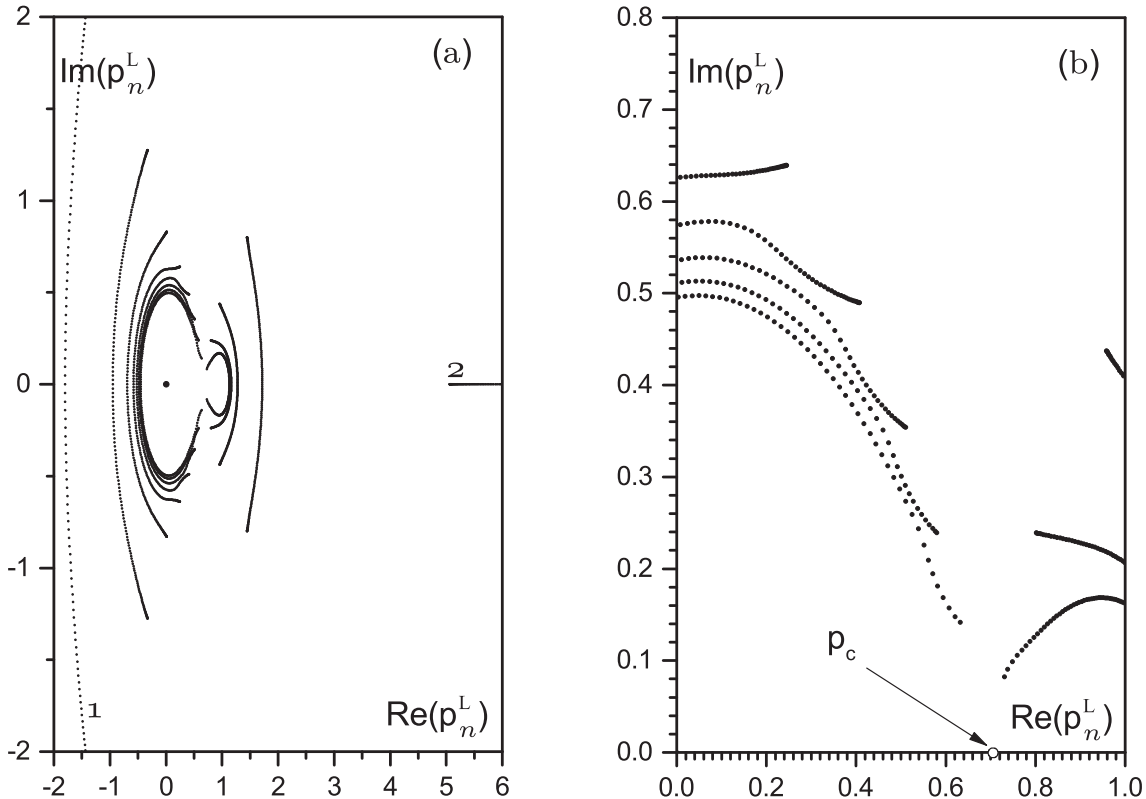
FIG. 3. Yang-Lee zeros for the survival probability $\mathcal{P}_{L,n}(p)$ corresponding to $n = 14$, $L = 200$. (a) Most of the Yang-Lee zeros p_n^L are located within the frame of this figure, with the exception of a small number of zeros following the lines denoted by 1 and 2 that fall outside the frame. (b) Portion of Yang-Lee zeros located in the region $0 < \mathrm{Re}(p_n^L) \leqslant 1$, $0 < \mathrm{Im}(p_n^L) < 0.8$; the arrow indicates the position of the real physical threshold p_c for directed site percolation on the square lattice [37,38].

increasing n. Such a behavior can be attributed to the onset of a phase transition that develops gradually on a large strip when both of its lengths n and L tend to infinity. Indeed, it is expected that derivative $d\mathcal{P}(p)/dp$ for a system on an infinite square lattice diverges as $p \to p_c$ from the above, where percolation threshold p_c is a well defined quantity. In the same limit, the survival probability should be (strictly) equal to zero in the region $p \leqslant p_c$. For finite systems percolation threshold is not precisely defined (due to rounding effects), but its value can be roughly approximated by positions of maxima of $d\mathcal{P}_{L,n}(p)/dp$ for sufficiently large n, and L. On the other hand, letting go $L \gg 1$ for a fixed n, positions of corresponding maxima tend to the point $p = 1$, reflecting essentially one-dimensional character of percolation phase transition on infinite strips having finite widths.

III. NUMERICAL APPROACH AND RESULTS

In this section we examine distribution of zeros of survival probability in the complex plane of occupation probability p. For moderate values of n and L, say $n \lesssim 15$, $L \lesssim 200$, $\mathcal{P}_{L,n}(p)$ can be obtained in analytical form using some of the available packages for symbolic computation. Since so generated expressions are polynomials, it is not difficult to calculate all zeros of $\mathcal{P}_{L,n}(p)$ for some given values of L and n. As a typical example, on the left panel of Fig. 3 we present a map of zeros of $\mathcal{P}_{L,n}(p)$ for $L = 200$ and $n = 14$. As one can infer from this picture, pattern of Yang-Lee zeros is rather complicated: It seems as if most zeros accumulate along a number of lines that move over the complex plane under a change of L. According to our numerical insights, number of these branches is fixed and equal to $n - 1$, for a given n. Since a new branch of zeros emerges each time we raise the width by 1, it is clear that the total number of these lines will grow to infinity for $n \to \infty$, which certainly reflects the complexity of directed percolation problem. In addition to these $n - 1$ loci of zeros, the point $p = 0$ represents a locus of zeros and accumulation point of these zeros, as a consequence of the fact that our survival probability allows the simple factorization: $\mathcal{P}_{L,n}(p) = p^L Q_{L,n}(p)$, where $Q_{L,n}(p)$ is a polynomial as well.

For better clarity, distribution of Y-L zeros in the region of physical interest, $0 < \text{Re}(p) \leqq 1$, is presented on the right panel of Fig. 3 for the same values of lattice parameters. Although much of complexity seen in the left panel is still present, one can also notice that the ending point of at least one branch of zeros seems to approach the real axis near the point of expected percolation threshold. Since one expects that the zero closest to the real positive axis, lying in the region $0 < \text{Re}(p) \leqq 1$, follows certain power-law behavior, our goal is to reveal and describe such a behavior in detail.

Before we continue our numerical analysis, it is worth mentioning that patterns of Yang-Lee zeros explored in previous studies of this problem [21,22] resemble those shown in Fig. 3. It is interesting, however, that associated maps of Y-L zeros for the sequence of survival probabilities obtained by method of series expansion, presented by polynomials of an increasing degree N, display surprisingly simple circularlike structure. According to our tests, first zeros of the sequence of such approximations, generated by using data of Ref. [32], seemingly approach the real axis near the point of expected

percolation threshold. Although at first glance this finding may seem promising, it is not of great help for computation of critical exponents by the Y-L method, which usually relies on some scaling laws for the first zeros, but there is no obvious way how to express them in terms of control variable N.

It is well known that the first zeros z_L of the partition function of an isotropic equilibrium system of linear size L usually display the simple leading asymptotic behavior [33]: $z_L \sim z_\infty + aL^{-1/\nu}$, where ν is the critical size exponent, z_∞ is the limiting zero corresponding to associated physical singularity, and a denotes a constant or at least a slowly varying function of L. The problem of a directed percolation is certainly more complicated, because one has to deal with two different lengths. One way to simplify the problem, in this context, is to take the limit $L \to \infty$ for a fixed n firstly, through a very large number $L \gg 1$ of iterations of (2), after which one is left with a system depending on n only. By analogy with the case of equilibrium systems, it seems reasonable to suppose that the first zeros p_n^∞ of $\mathcal{P}_{\infty,n}(p)$ for a strip of infinite length and finite but large width n, follow the asymptotic behavior

$$\text{Re}(p_n^\infty) = p_c + a_1 n^{-1/\nu^\perp}, \quad \text{Im}(p_n^\infty) = b_1 n^{-1/\nu^\perp}, \quad (4)$$

where a_1 and b_1 denote two real constants.

In order to use the above two relations for calculation of the percolation threshold p_c and the transverse-size critical exponent $\nu^\perp$ we need the values of $\text{Re}(p_n^\infty)$ and $\text{Im}(p_n^\infty)$. A rough estimates of these quantities, at least for strips of moderate widths, can be done straightforwardly by iterating the system (2) a large number of times. Direct computation that we performed in this way indicates that the first zeros p_n^L move more and more slowly towards the real axis by
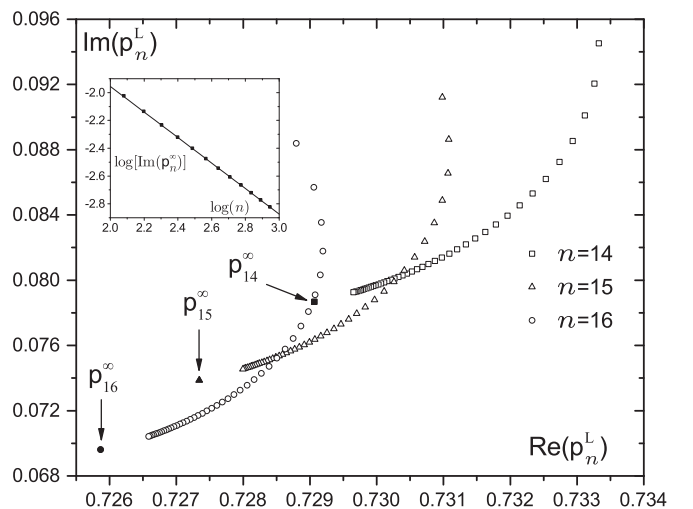
FIG. 4. Trajectories of the first Y-L zeros, i.e., sets of first zeros computed for a sequence of lengths $L_i = L_0 + i\Delta L$, $i = 1, 2, 3, \ldots, 42$, with $L_0 = 80$, $\Delta L = 10$, and $n = 14$, $n = 15$, and $n = 16$. Positions of the end points of these trajectories, corresponding to the limit $L \to \infty$, are indicated by solid symbols. To verify the scaling law (4), we presented $\log[\text{Im}(p_n^\infty)]$ as a function of $\log(n)$ in the inset, together with a straight line that provides the best fit to the last 12 data points; the slope of this line, $-1/\nu^\perp = -0.917(1)$, is in good agreement with accurate estimates of $\nu^\perp$.

TABLE I. The imaginary part $\mathrm{Im}(p)_0$ of the first zeros as function of L for fixed $n = 14$ (the second and the fourth column). For simplicity, these quantities are given here with 15 decimal places only, while we use at least 30 decimal places in the actual computation. Three sets of higher-order extrapolants, $\mathrm{Im}(p)_{14}$, $\mathrm{Im}(p)_{15}$, and $\mathrm{Im}(p)_{16}$, generated by successive applications of the BST procedure with $\omega = 1$, are shown. Values of the last 36 extrapolants, corresponding to the last seven sequences, rounded to 14 decimal places are indistinguishable: $\mathrm{Im}(p) = 0.07868513682378(2)$, where (2) refers to the error in the last digit, estimated by the BST procedure.

L	$\mathrm{Im}(p)_0$	L	$\mathrm{Im}(p)_0$	$\mathrm{Im}(p)_{14}$	$\mathrm{Im}(p)_{15}$	$\mathrm{Im}(p)_{16}$
250	0.080991807352257	380	0.079690840053705			
				0.07868513682707		
260	0.080823070430302	390	0.079639305807927		0.07868513682343	
				0.07868513682593		0.07868513682373
270	0.080671545711753	400	0.079591537910203		0.07868513682356	
				0.07868513682519		0.07868513682375
280	0.080535029112434	410	0.079547185109553		0.07868513682364	
				0.07868513682476		0.07868513682377
290	0.080411651776698	420	0.079505935534455		0.07868513682369	
				0.07868513682440		0.07868513682377
300	0.080299821526267	430	0.079467511578242		0.07868513682372	
				0.07868513682420		0.07868513682377
310	0.080198175792862	440	0.079431665535042		0.07868513682374	
				0.07868513682406		0.07868513682377
320	0.080105543545078	450	0.079398175864034		0.07868513682376	
				0.07868513682397		0.07868513682378
330	0.080020914309519	460	0.079366843981600		0.07868513682376	
				0.07868513682391		0.07868513682378
340	0.079943412824683	470	0.079337491498501		0.07868513682377	
				0.07868513682387		0.07868513682378
350	0.079872278194983	480	0.079309957833496		0.07868513682377	
				0.07868513682384		0.07868513682378
360	0.079806846661097	490	0.079284098146376		0.07868513682377	
				0.07868513682382		
370	0.079746537292514	500	0.079259781542874			

increasing gradually the number L of iterations. The computation based solely on the iteration method is not of great utility, in particular if one needs high precision of p_n^∞. The major cause of this problem is relatively slow convergence of the sequence p_n^L towards p_n^∞. As a consequence of slow convergence, one needs an extremely large number of iterations, which in turn require an enormous accuracy of the input data. For example, to ensure an accuracy of about ten significant digits for p_n^∞, one needs about 10^6 iterations and an accuracy of the input data of the same order of magnitude, making such a procedure practically intractable for larger values of n.

To circumvent the numerical difficulties we pointed out, and get good estimates of the required limiting values p_n^∞, in this work we compute the sequences p_n^L up to about $L = 500$, and, after that, we extrapolate them by using the Bulirisch-Stoer (BST) algorithm [34]. The advantage of the BST method over the other proposed extrapolation schemes, developed to accelerate the convergence of finite-size sequences, has been noticed in various studies of critical phenomena during the last two decades [35,36]. Concerning reliability and precision of extrapolated value of a given data sequence, it is clear that they depend primarily on the convergence properties of the sequence under consideration. But, as it was discussed in a work devoted to the application of BST algorithm to extrapolations of the sequences of Y-L zeros for the Ising model [36], accuracy of the obtained results depends to a great extent on the precision of the input data as well as on the

length of the sequence. To meet these conditions we generated rather long sequences of the Y-L zeros p_n^L, corresponding to the set of lattice lengths $i\Delta L$, with $\Delta L = 10$, and $i = 1, 2, 3, \ldots, 50$ typically. It turns out that for systems of these sizes, depending on the value of L, one needs an accuracy of the input data going up to 200 digits to get p_n^L to 30-figure accuracy; according to our observations, this accuracy is much less affected by values of n.

In Fig. 4 we presented trajectories of the first Y-L zeros for three typical values of n, and L going up to $L = 500$ in steps of length $\Delta L = 10$. The end points of these trajectories are computed by using the BST algorithm. Note that $\mathrm{Im}(p_n^L)$ is a decreasing function for all values of L, while $\mathrm{Re}(p_n^L)$ increases within an initial interval $L < \bar{L}(n)$ and decreases monotonically beyond this region. The values of $\bar{L}(n)$ slowly grow with n, and go up to about 160 for the system of the largest width $n = 19$ examined in this work. To avoid the region of nonmonotonic behavior of $\mathrm{Re}(p_n^L)$, in the application of the BST algorithm to the sequence $\mathrm{Re}(p_n^L)$, we excluded the set of values corresponding to the region $L < \bar{L}(n)$.

To give a flavor of the BST applicability in our case, we give some details of its application to the sequence $\mathrm{Im}(p_n^L)$, computed for $n = 14$, and denoted by $\mathrm{Im}(p)_0$ in Table I. After one application of the BST procedure to the initial sequence $\mathrm{Im}(p)_0$ one obtains the first sequence $\mathrm{Im}(p)_1$ of extrapolated data and this process continues iteratively, so that the sequence $\mathrm{Im}(p)_k$ is generated from the sequence $\mathrm{Im}(p)_{k-1}$

($k = 1, 2, 3, \ldots, 24$, in this example). As the iteration process proceeds, all extrapolated values become closer to each other. Since the BST algorithm includes subtraction of extrapolated values, its application to the high-order sequences causes a significant loss of accuracy, calling for an enhanced accuracy of the input data.

The method includes a free parameter ω, which has to be adjusted self-consistently in order to minimize the error and fluctuations in the new sequences of estimates generated by the BST algorithm. Difference between two extrapolated values of the next-to-last BST sequence is usually taken as a measure of the error of this procedure [35]. According to our observations, the best extrapolations with respect to L (n being fixed) are obtained for $\omega = 1$. Indeed, even some small changes of ω, $\omega = 1 \pm \epsilon$, $\epsilon \lesssim 10^{-2}$, lead to significant degradation of stability and convergence properties of all sequences, while the errors of the final extrapolants estimated by the BST procedure become much larger (by several orders of magnitude, typically). If one assumes that the leading finite-size correction term to $\mathrm{Im}(p_n^L)$ has the power-law form with some power ψ, $\mathrm{Im}(p_n^L) \sim \mathrm{Im}(p_n^\infty) + \mathrm{const.}/L^\psi$, then a single application of the BST algorithm eliminates this correction term providing the adjustable parameter ω is chosen to be equal to ψ. This strongly indicates that we have: $\mathrm{Im}(p_n^L) \sim \mathrm{Im}(p_n^\infty) + \mathrm{const.}/L$, which provides an additional confirmation of slow convergence of the sequences $\mathrm{Im}(p_n^L)$ and $\mathrm{Re}(p_n^L)$ that we mentioned above.

As one can infer from Table I, extrapolation procedure based on a sequence of 26 values of p_n^L works fairly well, giving a reliable and accurate estimate for $\mathrm{Im}(p_n^\infty)$. Precision of such estimates can be further enhanced by using longer sequences of accurate data. For this reason, all estimates presented in Table II are calculated through the sequences comprised of (at least) 35 different values.

The reliability of some of the BST estimates we also checked directly, through the simple brute-force computation. Of course, this can be done only for moderate values of n. Thus, for $n = 6$ and $n = 7$, we have been able to follow the evolution of the first zeros with iteration index L going up to more than 10^6, by setting accuracy of our input data to 5×10^5 significant digits. We have found that, indeed, these first zeros steadily approach corresponding values given in Table II. Let us note, however, that the value of the first zero, obtained after 1.5×10^6 iteration steps ($n = 6$), coincides with the BST value rounded to 12 decimal places. One would therefore need more than 10^9 iteration steps to reach the BST precision, which would be a difficult task for small and let alone for larger values of n.

Having determined the real parts of the first zeros in the limit $L \to \infty$, it is not difficult to get an estimate of the percolation threshold by using an extrapolation procedure to the sequence $\mathrm{Re}(p_n^\infty)$ of Table II. Thus, applying the BST algorithm to the data of the second column of this table, we get quite stable sets of extrapolants, which allow us to obtain a fairly accurate estimate of the percolation threshold, $p_c = 0.70548(1)$. This value is in agreement with more accurate estimate $p_c = 0.70548530(5)$ obtained through the transfer-matrix coupled with phenomenological renormalization group method [38]. Let us note, however, that the latter estimate has been obtained by using strips of widths going up to $n = 24$.

TABLE II. Real and imaginary parts of the limiting first Y-L zeros, $L \to \infty$, estimated through the BST procedure for fixed n. The sequence $v_n^\perp$ of finite width estimates, obtained through the relation (5), is shown in the fourth column. Our final BST estimates, together with the best choices of ω, are given in the last two rows. Note that the value of ω corresponding to the extrapolation of the sequences $\mathrm{Re}(p_n^\infty)$ and $\mathrm{Im}(p_n^\infty)$, $\omega = 0.91$, is very close to $1/v^\perp$, which is consistent with the scaling form (4).

n	$\mathrm{Re}(p_n^\infty)$	$\mathrm{Im}(p_n^\infty)$	$v_n^\perp$
5	0.793865926017881	0.207836151668583	
6	0.772811395253383	0.173859835806187	1.02140582748
7	0.759894687856575	0.149974180129320	1.04306484411
8	0.751180675057913	0.132183555112106	1.05749329439
9	0.744910464240068	0.118373603122745	1.06739959914
10	0.740183535535020	0.107316777244130	1.07444120067
11	0.736492340460778	0.098248704871143	1.07959922752
12	0.733529506167153	0.090667073810669	1.08347354098
13	0.731098195607174	0.084227403843044	1.08644534604
14	0.729066597126144	0.078685136823778	1.08876556533
15	0.727343155123767	0.073861605876756	1.09060451710
16	0.725862306538494	0.069623093925899	1.09208093536
17	0.724575873865141	0.065867440443035	1.09327954279
18	0.723447662646138	0.062515190593425	1.09426204067
19	0.722449954172795	0.059503579104875	1.09507418212
∞	0.70548(1)	0.00001(1)	1.096857(5)
ω	0.91	0.91	0.865

Due to simplicity of the second relation of (4), a rough estimate of the transverse-size critical exponent $v_n^\perp$ can be obtained directly, from the slope of straight line that best fits the set of points $[\log[\mathrm{Im}(p_n^\infty)], \log(n)]$; see inset of Fig. 4. Much better estimate of this quantities can be obtained from the relation

$$v_n^\perp = \frac{\log\left[\mathrm{Im}(p_n^\infty)/\mathrm{Im}(p_{n-1}^\infty)\right]}{\log[(n-1)/n]}, \qquad (5)$$

which we used to compute the sequence of finite-width estimates $v_n^\perp$ shown in the fourth column of Table II. To get an estimate corresponding to the thermodynamic limit $n \to \infty$, we apply the BST procedure to this data sequence, which leads to the final estimate $v^\perp = 1.096857(5)$. Note that this value of the transverse critical exponent is very close to the best currently available estimates for this quantity [37] $v^\perp = 1.096854(4)$ and [38] $v^\perp = 1.096822(2)$. It is perhaps surprising that, in our case, precision of transverse-size critical exponent exceeds that for the percolation threshold. Let us note, however, that the values of $v_n^\perp$ are noticeably closer to their limiting values $v^\perp$ if compared to the corresponding cases of $\mathrm{Re}(p_n^\infty)$ or $\mathrm{Im}(p_n^\infty)$ (see Table II). We believe that this difference stems from fact that $v_n^\perp$ is determined by the ratio (5), which eliminates dependence on parameter b_1 appearing in (4); for similar reason, it is also possible that the next-to-leading finite-size correction terms in $v_n^\perp$ are weaker than in the case of $\mathrm{Im}(p_n^\infty)$.

The approach that we used here can be, in principle, extended to the computation of longitudinal-size critical exponent $v^\parallel$. By analogy with the above procedure, one can

first compute the sequence of the first zeros for a fixed L, and, after that, make an extrapolation towards the limiting value p_∞^L. It is expected that the asymptotic form (4), with $\nu^\perp$ replaced by $\nu^\parallel$ and n replaced by L, is valid for p_∞^L. The main factor that limits practical realization of such a procedure is evidently the width n of the strips, since the transfer-matrix size grows exponentially with n. Nevertheless, we have been able to obtain a rough estimate of $\nu^\parallel$ by this method, which indicates its applicability although it is not so well suited for this purpose.

IV. CONCLUSION

In this paper we studied directed percolation problem on strips of the square lattice by using the method of Yang-Lee zeros. For this purpose we constructed transfer matrices for the sets of restricted probabilities which allow us to determine corresponding survival probabilities. After consideration of the maps of zeros of survival probabilities, we examined in detail scaling behavior of the first Y-L zeros. To avoid complexity related to the anisotropic scaling, we make extrapolation towards infinity in two steps: In the first step by letting the longitudinal length go to very large values $L \gg 1$, which is followed, in the second step, by an extrapolation towards large values of n. Thus, after the first step, one has to consider a simpler system, yielding to the natural scaling assumption (4) for a system having n as the only variable that controls its size. It seems that similar procedures can be useful in analysis of some other lattice models, in particular those involving more than one characteristic length.

In our efforts to build up percolation clusters of very large longitudinal lengths, and subsequent computation of the first Y-L zeros of associated survival probabilities, we have been faced with the problem of slow convergence. To handle the problem and get sufficient precision of limiting zeros, we use extensively the BST extrapolation procedure, validity of which has been justified by various means. In this way we have been able to obtain very accurate estimates of the transverse-size critical exponent $\nu^\perp$ and the percolation threshold p_c, meaning that the presented method is not only applicable but it can be even competitive with other

approaches aimed at getting accurate description of critical behavior.

APPENDIX: TRANSFER MATRIX

As a simple example we give here the recursion relation $\mathbf{P}_{L+1} = \mathbf{M}\mathbf{P}_L$ for restricted probabilities $P(\mathcal{C}_i)$ in the case of a strip of width $n = 5$. Due to symmetry of the system, the number of required configurations in this case can be reduced to seven states (instead of 31), as depicted in Fig. 5(a).

For a fixed configuration of sites at the column $L + 1$, one selects (from the set of all 31 possible states) all those configurations of the Lth column that ensure a connection of each occupied site of the right column (see Fig. 1). After finding an allowed pair of configurations, one associates the weight p to each occupied site of the right configuration, and weight q to each perimeter site, i.e., to each empty site of the right column providing that it has an occupied predecessor at the left column. This procedure is illustrated in Fig. 5(b), where we show how to obtain the matrix element $\mathbf{M}_{54}$. By analogy, one can obtain all other matrix elements and verify that the transfer matrix $\mathbf{M}$ has the form

$$
\begin{pmatrix}
p^5 & 0 & 0 & 0 & 0 & 5p^5 & 5p^5 \\
pq^4 & 2pq & 3pq^2 & 4pq^3 & 4pq^3 & 5pq^4 & 5pq^4 \\
p^2q^3 & p^2 & 2p^2q & 3p^2q^2 & 3p^2q^2 & 5p^2q^3 & 5p^2q^3 \\
p^2q^3 & 0 & p^2q & 3p^2q^2 & 3p^2q^2 & 5p^2q^3 & 5p^2q^3 \\
p^3q^2 & 0 & p^3 & 2p^3q & 2p^3q & 5p^3q^2 & 5p^3q^2 \\
p^3q^2 & 0 & 0 & 2p^3q & 2p^3q & 5p^3q^2 & 5p^3q^2 \\
p^4q & 0 & 0 & p^4 & p^4 & 5p^4q & 5p^4q
\end{pmatrix},
$$

$$(A1)$$
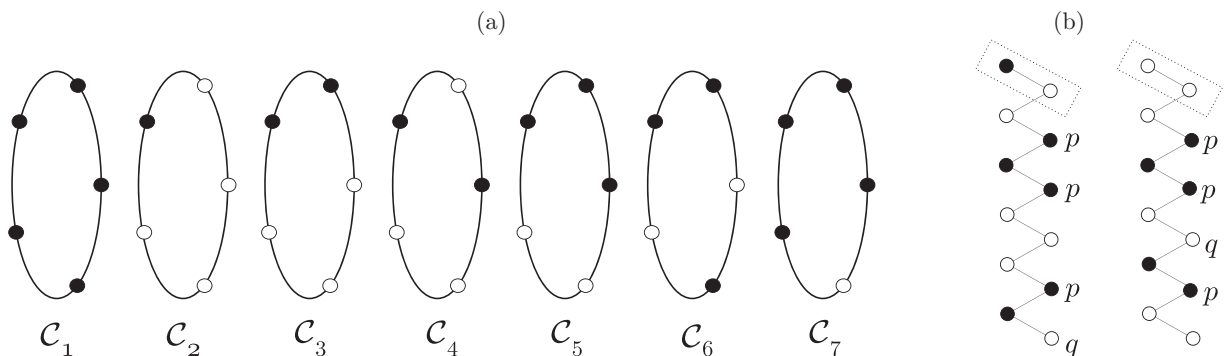
FIG. 5. (a) Schematic representation of column states on a strip of width $n = 5$, described via seven configurations of empty (open circles) and occupied sites (filled circles). One associates a restricted probability $P(\mathcal{C}_i)$ to each cluster ending with configuration $\mathcal{C}_i$. (b) There are two allowed $\mathcal{C}_4$ configurations (left columns) giving rise to the matrix element $\mathbf{M}_{54} = 2p^3q$ that appears in recursion relation for $P(\mathcal{C}_5)$ ($\mathcal{C}_5$ is presented by right columns). Due to periodic boundary conditions, two top pairs of sites (enclosed by two rectangles) should be identified with two corresponding pairs of sites at the bottom of the figure.

providing that the components of state vector has been chosen so that they follow the order of states as depicted in Fig. 5(a),

$$\mathbf{P}_L = (P_1, P_2, P_3, P_4, P_5, P_6, P_7)^T, \tag{A2}$$

where P_i, $i = 1, 2, \ldots, 7$, denotes restricted probability $P(\mathcal{C}_i)$ for a strip of length L (we omitted index L), and similarly in the case of vector $\mathbf{P}_{L+1}$. It is also easy to see that the state $\mathcal{C}_1$ is unique, $d(\mathcal{C}_1) = 1$, while all other states ($i \neq 1$) have $d(\mathcal{C}_i) = 5$ different ways to be embedded into a column of width $n = 5$.

[1] C. N. Yang and T. D. Lee, Statistical theory of equations of state and phase transitions. I Theory of condensation, Phys. Rev. **87**, 404 (1952).

[2] T. D. Lee and C. N. Yang, Statistical theory of equations of state and phase transitions. II Lattice gas and Ising model, Phys. Rev. **87**, 410 (1952).

[3] M. E. Fisher, in *Lectures in Theoretical Physics*, edited by W. E. Brittin (University of Colorado Press, Boulder, 1965), Vol. 7C, Chap. 1.

[4] D. A. Kurtze, M. S. C. Report No. 4184, Cornell University, 1979 (unpublished).

[5] I. Bena, M. Droz, and A. Lipowski, Statistical mechanics of equilibrium and nonequilibrium phase transitions: The Yang-Lee formalism, Int. J. Mod. Phys. B **19**, 4269 (2005).

[6] V. Privman and D. A. Kurtze, Partition function zeros in two-dimensional lattice models of the polymer Θ-point, Macromolecules **19**, 2377 (1986).

[7] J. H. Lee, S. Y. Kim, and J. Lee, Exact partition function zeros of a polymer on a simple cubic lattice, Phys. Rev. E **86**, 011802 (2012).

[8] J. H. Lee, S. Y. Kim, and J. Lee, Partition function zeros of a square-lattice homopolymer with nearest and next-nearest-neighbor interactions, Phys. Rev. E **87**, 052601 (2013).

[9] J. C. S. Rocha, S. Schnabel, D. Landau, and M. Bachmann, Identifying transitions in finite systems by means of partition function zeros and microcanonical inflection-point analysis: A comparison for elastic flexible polymers, Phys. Rev. E **90**, 022601 (2014).

[10] M. P. Taylor, P. P. Aung, and W. Paul, Partition function zeros and phase transitions for a square-well polymer chain, Phys. Rev. E **88**, 012604 (2013).

[11] M. P. Taylor and J. Luettmer-Strathmann, Partition function zeros and finite size scaling for polymer adsorption, J. Chem. Phys. **141**, 204906 (2014).

[12] E. J. Janse van Rensburg, Partition and generating function zeros in adsorbing self-avoiding walks, J. Stat. Mech. (2017) 033208.

[13] M. Knežević and M. Knežević, Polymer collapse transition: a view from the complex fugacity plane, J. Phys. A **52**, 125002 (2019).

[14] J. Lee, Exact Partition Function Zeros of the Wako-Saitô-Muñoz-Seato Protein Model, Phys. Rev. Lett. **110**, 248101 (2013).

[15] A. Deger, K. Brandner, and C. Flindt, Lee-Yang zeros and large-deviation statistics of a molecular zipper, Phys. Rev. E **97**, 012115 (2018).

[16] R. A. Blythe and M. R. Evans, The Lee-Yang theory of equilibrium and nonequilibrium phase transitions, Braz. J. Phys. **33**, 464 (2003).

[17] P. F. Arndt, Yang-Lee Theory for a Nonequilibrium Phase Transition, Phys. Rev. Lett. **84**, 814 (2000).

[18] R. A. Blythe and M. R. Evans, Lee-Yang Zeros and Phase Transitions in Nonequilibrium Steady States, Phys. Rev. Lett. **89**, 080601 (2002).

[19] F. H. Jafarpour, The application of the Yang-Lee theory to study a phase transition in a non-equilibrium system, J. Stat. Phys. **113**, 269 (2003).

[20] F. H. Jafarpour, First-order phase transitions in a reaction-diffusion model with open boundary: The Yang-Lee theory, J. Phys. A **36**, 7497 (2003).

[21] P. F. Arndt, S. R. Dahmen, and H. Hinrichsen, Directed percolation, fractal roots and the Lee-Yang theorem, Physica A (Amsterdam) **295**, 128 (2001).

[22] S. M. Dammer, S. R. Dahmen, and H. Hinrichsen, Yang-Lee zeros for a nonequilibrium phase transition, J. Phys. A **35**, 4527 (2002).

[23] M. Heyl, A. Polkovnikov, and S. Kehrein, Dynamical Quantum Phase Transitions in the Transverse-Field Ising Model, Phys. Rev. Lett. **110**, 135704 (2013).

[24] K. P. Gnatenko, A. Kargol, and V. M. Tkachuk, Two-time correlation functions and the Lee-Yang zeros for an interacting Bose gas, Phys. Rev. E **96**, 032116 (2017).

[25] C. Binek, Density of Zeros on the Lee-Yang Circle Obtained from Magnetization Data of a Two-Dimensional Ising Ferromagnet, Phys. Rev. Lett. **81**, 5644 (1998).

[26] C. Binek, *Ising-type Antiferromagnets: Model Systems in Statistical Physics and in the Magnetism of Exchange Bias*, 1st ed. (Springer-Verlag, Berlin, 2003).

[27] B.-B. Wei and R.-B. Liu, Lee-Yang Zeros and Critical Times in Decoherence of a Probe Spin Coupled to a Bath, Phys. Rev. Lett. **109**, 185701 (2012).

[28] X. Peng, H. Zhou, B.-B. Wei, J. Cui, J. Du, and R.-B. Liu, Experimental Observation of Lee-Yang Zeros, Phys. Rev. Lett. **114**, 010601 (2015).

[29] K. Brandner, V. F. Maisi, J. P. Pekola, J. P. Garrahan, and C. Flindt, Experimental Determination of Dynamical Lee-Yang Zeros, Phys. Rev. Lett. **118**, 180601 (2017).

[30] K. P. Gnatenko, A. Kargol, and V. M. Tkachuk, Lee-Yang zeros and two-time spin correlation function, Physica A (Amsterdam) **509**, 1095 (2018).

[31] H. Hinrichsen, Nonequilibrium critical phenomena and phase transitions into absorbing states, Adv. Phys. **49**, 815 (2000).

[32] I. Jensen and A. J. Guttmann, Series expansions of the percolation probability for directed square and honeycomb lattices, J. Phys. A **28**, 4813 (1995).

[33] C. Itzykson, R. B. Pearson, and J. B. Zuber, Distribution of zeros in Ising and gauge models, Nucl. Phys. B **220**, 415 (1983).

[34] R. Bulirsch and J. Stoer, Fehlerabschätzungen und extrapolation mit rationalen funktionen bei verfahren vom Richardson-typus, Numer. Math. **6**, 413 (1964).

[35] M. Henkel and G. Schütz, Finite-lattice extrapolation algorithms, J. Phys. A **21**, 2617 (1988).

[36] J. L. Monroe, Extrapolation and Bulirsch-Stoer algorithm, Phys. Rev. E **65**, 066116 (2002).

[37] I. Jensen, Low-density series expansions for directed percolation: I. A new efficient algorithm with applications to the square lattice, J. Phys. A **32**, 5233 (1999).

[38] D. Knežević and M. Knežević, A transfer-matrix study of directed lattice animals and directed percolation on a square lattice, J. Phys. A **49**, 115001 (2016).